Pd Nanoparticles Supported on Hydrotalcite-modified Porous Alumina Spheres as Selective Hydrogenation Catalyst

Fazhi Zhang, Jiali Chen, Peng Chen, Zhiyi Sun, and Sailong Xu
State Key Laboratory of Chemical Resource Engineering, Beijing University of Chemical Technology, Beijing 100029, China

DOI 10.1002/aic.12694
Published online June 20, 2011 in Wiley Online Library (wileyonlinelibrary.com).

The immobilization or supporting of transition-metal nanoparticles on carriers by different techniques has attracted much attention, considering the significance of nanocatalysts in actual practical applications. Here we report Pd nanoparticles supported on modified porous θ-alumina spheres are adopted as heterogeneous catalysts for the selective hydrogenation of dimethyl terephthalate (DMT) to dimethyl cyclohexane-1,4-dicarboxylate (DMCD), a kind of significant polymer modification and intermediate. θ-alumina spheres as supports were originally modified by in situ *growth of magnesium-aluminum layered double hydroxide (MgAl-LDH; also known as hydrotalcite) in the pores and on the surface. Pd nanoparticles were immobilized on the supports by a subsequent wet impregnating method. The resulting Pd nanoparticles catalyst provides quite higher activity/selectivity compared with that supported on the unmodified alumina spheres with the same loading of Pd. The enhanced catalytic performance of the former can be ascribed to the higher dispersion of Pd nanoparticles and the smaller particle size.* © 2011 American Institute of Chemical Engineers *AIChE J,* 58: 1853–1861, 2012
Keywords: Palladium, selective hydrogenation, dimethyl terephthalate, dimethyl cyclohexane-1, 4-dicarboxylate, layered double hydroxide

Introduction

1,4-cyclohexanedimethanol (CHDM), as a linker molecular in the polymer industry, is a highly valued and significantly used reagent.[1] For instance, as the stepping stone, CHDM is preferred to ethylene glycol in the production of polyester fibers for applications involving polycarbonates and polyurethane. It is prepared industrially by a two process using two reactors. The first step is the highly exothermic conversion of DMT into DMCD by using a supported Pd catalyst in the temperature range of 160–180°C, and an H_2 pressure of 30–48 MPa. The intermediate DMCD is then converted into CHDM by using a copper-chromite catalyst at temperatures about 200°C and an H_2 pressure of about 4 MPa (Scheme 1).[2,3] With regard to the selective hydrogenation of DMT, many procedures using catalysts such as Pd, Ru, Ni-based ones have so far been reported, however, only Pd catalyst has been practically industrial applied. Recently, Thomas and coworkers reported that a bimetallic nanoparticle catalysts,[4] such as (silica-supported) Ru_5Pt, $Ru_{10}Pt_2$, Ru_6Pd_6, and $Ru_{12}Cu_4$, and a trimetallic cluster Ru_5PtSn,[5] can promote the single step conversion of DMT into CHDM under mild reaction conditions.

Pd is well known as active component of hydrogenation catalysts in many reaction processes with high-catalytic activity and poisoning-resistance.[6,7] Conventionally, supported Pd catalysts are prepared by impregnating using different porous materials as supports in aqueous solutions containing

Correspondence concerning this article should be addressed to F. Zhang at zhangfz@mail.buct.edu.cn.

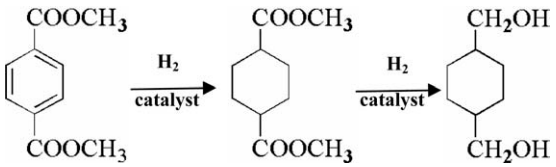

Scheme 1. Preparation of CHDM industrially by a two process.

active Pd precursors. The properties of Pd catalysts prepared by this method are not fully reproducible because of high-surface tension of water. The most evident fact is to lead to inhomogeneity in distribution of the Pd particles supported. Moreover, this inhomogeneity will be usually enhanced during the calcination process at high temperature. Nowadays, it remains a challenge to synthesize Pd catalyst with high dispersion for actual practical applications.[8–11]

Layered double hydroxides (LDHs), also known as hydrotalcite-like materials, are a class of anionic clays whose structure is based on brucite ($Mg(OH)_2$)-like layers in which some of the divalent cations have been replaced by trivalent ions giving positively-charged sheets.[12,13] The flexibility in composition allows LDHs with an interesting opportunity for developing new catalysts, catalyst precursors, or catalyst supports with a tailored structure-design, controlled accessibility to the catalytic sites and properties.[14–18] According to literature, in most relevant work of the combination of metal active components and hydrotalcite reported so far, hydrotalcite which promotes the deposition, separation and dispersion of the active ones plays an essential role in the enhancement of catalytic activity and selectivity and offers the assistant activation potentials for some reactions.[19–25] For instance, Ru-grafted catalysts obtained from the treatment of Ru precursors and hydrotalcite supports enhance the transformation of direct α-alkylation of nitriles with primary alcohols.[19] A robust heterotrimetallic $RuMn_2$/HT which is uniform in composition and distribution was fabricated by coordination of the catalytically active compounds to a hydrotalcite surface.[20] This material is an excellent solid catalyst for liquid-phase alcohol oxidation with molecular oxygen under mild conditions. By taking advantage of this feature it should be possible to modify the properties of the supported Pd catalysts by deposition of the active Pd component on the hydrotalcite surface, and, hence, fabricate a Pd nanoparticle catalyst with high distribution.[25]

Herein, we report Pd nanoparticles supported on hydrotalcite-modified porous alumina particles are adopted as heterogeneous catalysts for selective hydrogenation. Inspired by the phenomenon of NiAl-LDHs coprecipitation formed by impregnation of γ-alumina with Ni^{2+} at neutral or near neutral pH and ambient temperature,[26,27] the porous θ-alumina with high-specific surface area and excellent physical strength was used as a support and sole source of Al^{3+} for the *in situ* growth of MgAl-LDHs in the pores and on the surface. The *in situ* synthesis of LDHs was carried out by decomposition of urea dissolved in an aqueous solution of Mg^{2+} impregnated into Al_2O_3. After a subsequent impregnation of Pd precursor, a highly dispersed Pd nanoparticles catalyst was obtained. For comparison, two catalyst samples with the same Pd loading with or without Mg as assistant component (denoted as Pd-Mg/Al_2O_3 and Pd/Al_2O_3, respectively) were prepared by impregnating using unmodified alumina supports in aqueous solutions containing active metal precursor. The structure, morphology, and texture features of the resulting catalysts, as well as the catalytic performance in the selective hydrogenation of DMT to DMCD, were investigated.

Experimental

Materials

$PdCl_2$, NaCl, $Mg(NO_3)_2{\cdot}6H_2O$, $CO(NH_2)_2$, hydrochloric acid and dimethyl terephthalate (DMT) were all of A.R. grade and used without further purification. The porous θ-alumina spheres with a purity of 99.5% prepared in our laboratory were carefully crushed into particles with an average particle size of 20–40 mesh before used as supports. The deionized water with a conductance below 10^{-6} S/cm was used in all synthesis and washing processes.

Preparation of hydrotalcite-modified porous alumina spheres

The *in situ* growth method was used in the synthesis of hydrotalcite-modified θ-alumina particles.[28,29] Porous θ-alumina 2.0 g was put into a stainless steel autoclave (100 mL in volume) with a Teflon lining, to which a solution of urea (0.16 mol) in water (12 mL) was added. The autoclave was heated at 90°C for 24 h. $Mg(NO_3)_2{\cdot}6H_2O$ (0.04 mol) was subsequently introduced into the autoclave which was heated at 130°C for 24 h. The resulting sample was denoted as HT-Al_2O_3. HT-Al_2O_3 sample was calcined at 450°C for 6 h and denoted as HT_C-Al_2O_3.

Preparation of Pd supported catalysts

HT-Al_2O_3 sample was calcined at 450°C for 6 h and denoted as HT_C-Al_2O_3. Pd supported catalyst with Pd loading 0.3 wt % was obtained by subsequent wet impregnating an aqueous solution of $PdCl_2$ precursor with the HT_C-Al_2O_3 supports, followed by the essential thermal treatment. The sample obtained was

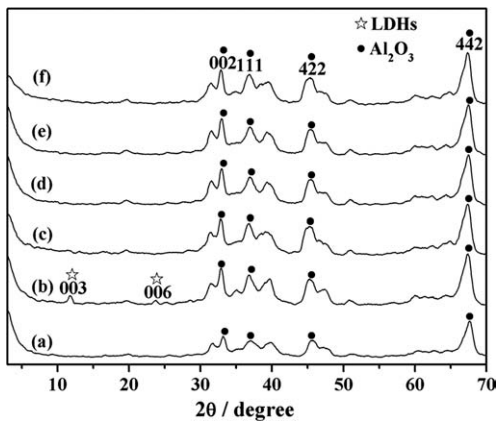

Figure 1. Powder XRD patterns for porous θ-Al_2O_3 sphere (a), HT-Al_2O_3 (b), HT_C-Al_2O_3 (c), and Pd/HT_C-Al_2O_3 (d), Pd/Al_2O_3 (e) and Pd-Mg/Al_2O_3 (f) samples, fabricated by impregnating using unmodified porous θ-alumina supports are shown for comparison.

Table 1. Physicalchemical Properties of Samples

Samples	HT-Al_2O_3	Pd/HT_C-Al_2O_3	Pd/Al_2O_3	Pd-Mg/Al_2O_3
Loading weights of Pd[#]/wt%	/	0.29	0.28	0.29
Loading weights of Mg[#]/wt%	0.98	0.96	/	0.97
Pd dispersion[&]/%	/	38.2	25.1	30.4

[#]Value determined by ICP.
[&]Value calculated based on the H_2-TPR/TPD.

denoted as Pd/HT_C-Al_2O_3. For comparison, supported 0.3 wt % Pd catalysts with or without Mg as assistant component (denoted as Pd-Mg/Al_2O_3 and Pd/Al_2O_3, respectively) were prepared by impregnating using unmodified porous θ-alumina supports in aqueous solutions containing active metal precursor.

Characterization

Power X-ray diffraction (XRD) patterns were collected on a Shimadzu XRD-6000 X-ray diffractometer with Cu Kα radiation ($\lambda = 0.154$ nm) at 40 kV, 30 mA, a 2θ angle ranging from 3 to 70°, and a scanning rate of 10°/min, a step size of 0.02°/s. Elemental analysis of samples was carried out by inductively coupled plasma-atomic emission spectrometry (ICP-ES) using a Shimadzu ICP-7500 instrument. The morphology, grain size of the samples and Pd elemental distribution were observed and monitored by scanning electron micrograph (SEM), and energy-dispersive X-ray (EDX) analysis using a Zeiss Supra55 system. The Pd nanoparticles dispersion was observed by an JEM-3010 high-resolution transmission electron microscopy (HRTEM). Low-temperature N_2 adsorption-desorption experiments were carried out using the Qutantachrome Autosorb-1C-VP instrument. The Barrett-Joyner-Halenda (BJH) method was used to calculate the pore volume and the pore-size distribution. The bulk density of samples was achieved by calculating the average value of certain amount randomly chosen particles.

The basic dispersion of the solid catalysts was investigated by temperature programmed reduction (TPR), and hydrogen temperature programmed desorption (H_2-TPD) with a Micromeritics ChemiSorb 2720, and the procedure was as follows: prior to the reduction of the catalysts, the sample was cleaned by passing an N_2 stream with a rate of 40 mL/min at 200°C for 2 h in order to remove any physisorbed molecules, and then the stream of 10% H_2 in Ar was injected by the same flow rate as before with a heating ramp rate 10°C/min. Simultaneously, the outlet gas was passed through a cold trap to remove the moisture produced during reduction, then the adsorption of the reduced samples was finished by 10% H_2 in Ar. Once a stable baseline was obtained, chemisorbed H_2 was desorbed by programmed heating at a rate of 10°C/min, and subsequently, the desorption process were finished. All the signals were calibrated using Ag_2O as the standard. The specific dispersion of Pd was calculated based on the volume of H_2 chemisorbed using the following simplified equation

$$\text{Pd dispersion (D)} : \mathrm{D} = \frac{2Vad}{Ws} \cdot \frac{FW}{F} \cdot \frac{SF}{Vm} \cdot 100\%$$

where *Vad* (mL) denotes the chemisorbed volume of H_2 at standard temperature and pressure (STP) conditions to form a monolayer in the TPD procedure, *Ws* the weight of samples (g), *FW* the formula weight of Pd (106.42 g/mol), *F* weight fraction of Pd in the sample as determined by ICP, *SF* stoichiometric factor (the Pd:H molar ratio in the chemisorption) which is taken as 1 and *Vm* is molar volume of H_2 (22414 mL/mol) at STP.

Catalytic reaction procedure

All the selective hydrogenation reactions were carried out in a stainless fixed-bed microreactor connected to the H_2 and N_2 cylinders. After the catalyst sample (3.5 mL) was placed in the static bed under a N_2 atmosphere, the atmosphere was replaced by H_2, and then the sample was reduced at 300°C for 2 h. After the reduction was finished, the static bed was cooled to the required temperature with the continuously injected reactants DMT, simultaneously, the hydrogen pressure in the reactor was adjusted to the required pressure while the H_2/DMT molar ratio, that is, 120, was retained, then the reaction was started and the products were analyzed by GC-2014C (Shimadzu, Japan) equipped with a Rtx-5 chromatographic column, a flame ionizing detector (FID) and identified by comparison of their mass spectra with those of authentic samples. The main byproducts are 4-methyl-1-cyclohexanecarboxylate and 4-methyl-1-methyl benzecarboxylate. Therefore, the specific catalytic performances were expressed by the following simplified equation

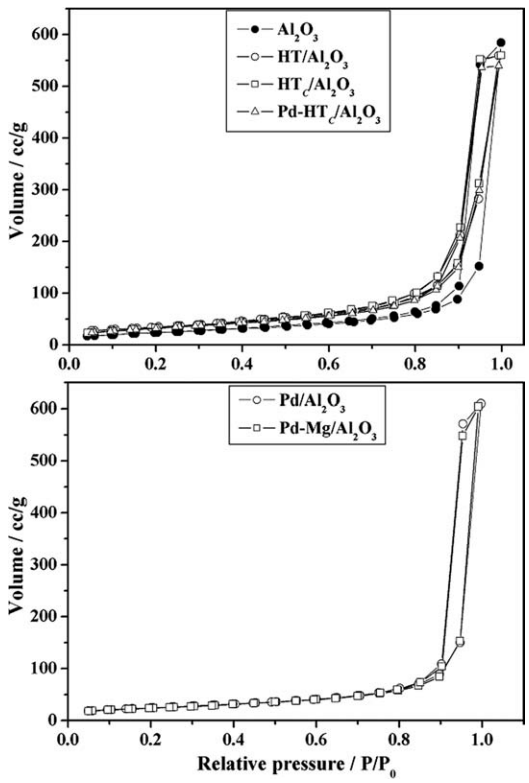

Figure 2. N_2 adsorption-desorption isotherms of porous θ-Al_2O_3 sphere, HT-Al_2O_3, HT_C-Al_2O_3, Pd/HT_C-Al_2O_3, Pd/Al_2O_3, and Pd-Mg/Al_2O_3.

Table 2. Textural Properties of the Samples

Samples	Bulk density (g/ml)	Specific surface area (m^2/g)	Most probable pore size (nm)	Total pore volume (cc/g)
θ-Al_2O_3	0.497	82.7	32.8	1.16
HT-Al_2O_3	0.531	91.7	32.1	1.03
HT_C-Al_2O_3	0.529	99.1	31.8	0.94
Pd/HT_C-Al_2O_3	0.565	90.4	30.1	0.92
Pd-Mg/Al_2O_3*	0.545	85.5	32.8	0.93
Pd/Al_2O_3*	0.524	83.4	31.8	0.94

*Prepared by impregnating using unmodified porous θ-alumina supports.

$$C = \left(1 - \frac{R_{DMT}A_{DMT}}{R_{DMT}A_{DMT} + R_{DMCD}A_{DMCD} + \sum_{i=1}^{n} R_iA_i}\right) \times 100\%$$

$$S = \frac{R_{DMCD}A_{DMCD}}{R_{DMCD}A_{DMCD} + \sum_{i=1}^{n} R_iA_i} \times 100\%$$

where C is catalytic conversion of DMT (%), S catalytic selectivity of main product DMCD (%), i a certain byproduct, R the relative area rectifying factor, and A denotes area percentage as determined by GC-2014C.

Results and Discussion

Composition and texture of catalysts

The powder XRD patterns for θ-Al_2O_3, HT-Al_2O_3, HT_C-Al_2O_3, and Pd/HT_C-Al_2O_3 are shown in Figure 1a–d, respectively. The characteristic reflections (002), (111), (422) and (442) of θ-Al_2O_3 are essentially similar for the four samples, which indicates that the initial support was mainly preserved despite some treatments. Simultaneously, the marked peaks (003) and (006) in Figure 1b, attached to the typical structure of LDHs and disappearing in succeeding curves Figure 1c and after thermal treatment, are similar to those reported in the literature for LDH phase.[30,31] Moreover, the characteristic peaks of HT-Al_2O_3 obtained are a superposition of the typical reflections of the θ-Al_2O_3 and LDHs phases. It is confirmed that the growth of MgAl-LDHs was carried out on the θ-Al_2O_3 support. Also, we mention that no characteristic diffraction peaks of Pd can be observed for the Pd/HT_C-Al_2O_3 (Figure 1d) and two Pd catalyst samples fabricated by impregnating using unmodified porous θ-alumina supports (Figure 1e and f) for the low Pd loading of about 0.3 wt %.

The exact Pd and Mg loading determined by ICP are listed in Table 1. The Pd loading in the three catalyst samples is almost the same. Also, the value of the Mg loading in Pd/HT_C-Al_2O_3 is very similar to that in the HT-Al_2O_3 and Pd-Mg/Al_2O_3.

The N_2 adsorption-desorption isotherms of the six samples are shown in Figure 2. All the isotherms of the samples are Type IV with an obvious hysteresis loop. In each case, the shape of the hysteresis loop was a superposition of Type H1 and H3, which is generally taken to indicate that the relevant samples have both parallel and tubular slit-shaped capillary pores caused by the gas escaping during calcinations and the stacking of alumina and MgAl-LDHs microcrystallites.[32,33] The corresponding specific textural properties of the six samples are listed in Table 2. As shown in Figure 2, compared to the pristine porous θ-Al_2O_3 sample, the volume value of the HT/Al_2O_3 sample moves toward higher at the same P/P_0, whereas at the highest P/P_0 the volume decreases. This may due to the *in situ* formation of MgAl-LDHs microcrystallites, leading to the higher surface area and aggregated block for some pores in the θ-Al_2O_3 sample. Similarly, such tendency of movements were also observed for HT_C-Al_2O_3 by calcination of HT-Al_2O_3, as that reported previously for the transformation of LDHs to the mixed metal oxide by calcination.[23,34] The increase of the specific surface area for the three samples can be seen in Table 2.

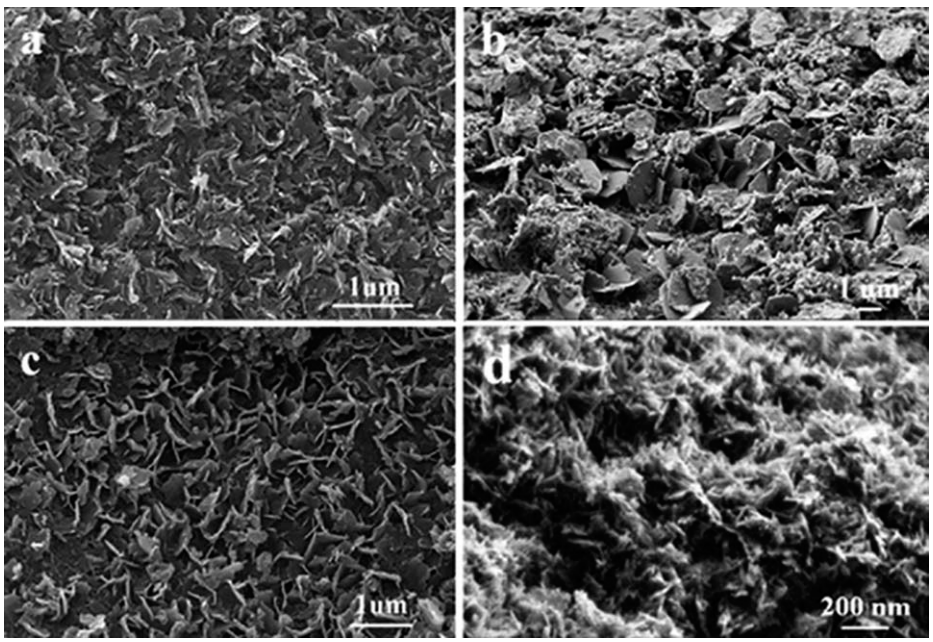

Figure 3. Representative SEM images of sample surface of porous θ-Al_2O_3 (a), HT-Al_2O_3 (b), Pd/HT_C-Al_2O_3 (c), and the cross section of HT-Al_2O_3 (d).

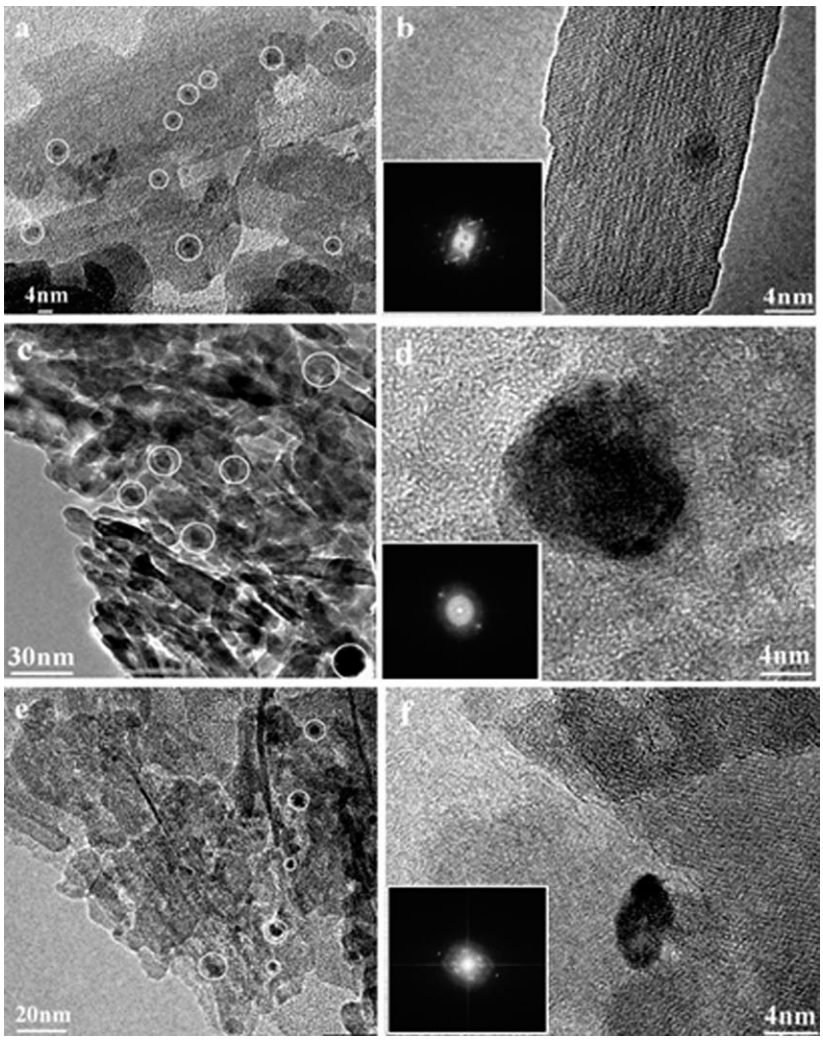

Figure 4. Representative HRTEM images of Pd/HT_C-Al_2O_3 (a), Pd/Al_2O_3 (c), and Pd-Mg/Al_2O_3 (e). (b), (d), and (f) shows a high-magnification view of (a), (c), and (e), respectively.

Inset shows the corresponding electron beam diffraction.

Furthermore, the subsequent Pd impregnation for Pd/HT_C-Al_2O_3 sample unavoidably slightly decreased the movements referred before, caused by aggregation and block of Pd precursors on the surface and in the pores during the impregnation. The two catalysts Pd/Al_2O_3 and Pd-Mg/Al_2O_3, prepared by impregnating using unmodified porous θ-alumina supports, almost provides the consistent isotherms, indicating the existence of similar textural structure. Generally, the corresponding textural properties including bulk density, specific surface area, most probable pore size, and total pore volume are listed in Table 2. There exist the significant differences in the series of samples θ-Al_2O_3, HT-Al_2O_3, HT_C-Al_2O_3, and Pd/HT_C-Al_2O_3, including the increased surface area and bulk density as a whole and the inevitably reduced most probable pore size and total volume ascribed to the injection and block in the pore. The aforementioned results indicate the distinct improvement in the architecture by modification, which is attributed to the growth of MgAl-LDHs microcrystallites on the surfaces and in the pores of Al_2O_3 domain by the *in situ* procedure. The improvement in the architecture would be beneficial to the dispersed deposition of Pd nanoparticles. Compared with the impregnated Pd/Al_2O_3 and Pd-Mg/Al_2O_3, Pd/HT_C-Al_2O_3 has slightly higher surface area and smaller most probable pore size.

Morphology and Pd particles size of catalysts

The representative SEM images of θ-Al_2O_3 and HT-Al_2O_3 (Figure 3a and b) directly give us the evidence for the formation of hydrotalcite microcrystallites by the *in situ* growth. For the HT-Al_2O_3 sample (Figure 3b and d), hydrotalcite microcrystallites having good crystallinity and uniform size grew homogeneously in the pores and on the surface of θ-Al_2O_3. The crystallite size of hydrotalcite in the *c*-direction was 3-6 nm. After subsequent calcination and impregnation of Pd precursors, we can also observe the hydrotalcite platelets on the surface and in the pores of Al_2O_3 support.

The HRTEM images of Pd/HT_C-Al_2O_3, Pd/Al_2O_3, and Pd-Mg/Al_2O_3 (Figure 4) clearly reveal the supported Pd nanoparticles have significantly different particle size on the

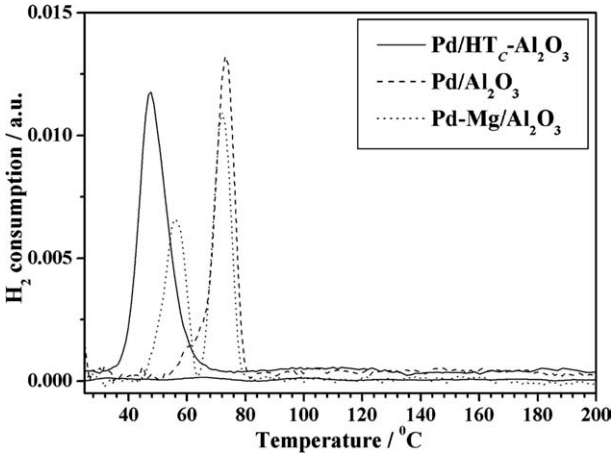

Figure 5. H_2-TPR profiles of Pd/HT_C-Al_2O_3, Pd/Al_2O_3, and Pd-Mg/Al_2O_3.

different supports. Pd/HT_C-Al_2O_3 has the smallest mean Pd particle size of about 4 nm (Figure 4a). While, for the Pd/Al_2O_3 and Pd-Mg/Al_2O_3 samples, the Pd metal particles are found to be agglomerated and the mean particle size are about 12 nm and 7 nm, respectively (Figure 4c and e). Figure 4b corresponds to a representative HRTEM image for the characterization of individual particles in the case of Pd/HT_C-Al_2O_3 sample. Particle with a diameter of ca. 4 nm, exhibits lattice fringes at 2.16 and 2.63 Å, which are ascribed to (110) and (101) planes of PdO (nominal value 2.14 and 2.63 Å, respectively; see the electron beam diffraction in the corresponding inset). The results give the direct evidence of the presence of highly dispersed Pd nanoparticles with small particle size in the Pd/HT_C-Al_2O_3 sample, which may have an essential effect on the development of selective hydrogenation.

Reducibility of catalysts

The H_2-TPR curves of Pd/HT_C-Al_2O_3, Pd/Al_2O_3, and Pd-Mg/Al_2O_3 (Figure 5) distinctly display the different reduction performance for the Pd catalysts supported on the different supports. The Pd/HT_C-Al_2O_3 sample with modified Al_2O_3 support has a single reduced temperature around 47.4°C; while for the Pd/Al_2O_3 the reduced temperature is ca.72.8°C. The Pd-Mg/Al_2O_3 sample, however, has two reduction peaks at ca. 71.9°C and 56.2°C, respectively. The presence of multiple reduction peaks may be ascribe to the uneven segregation of Pd nanoparticles for the sake of coimpregnation process, resulting from the migration of Mg to the Pd nanoparticles and interacting differently with the support as that reported for Li, Ca and Sr-promoted Pd catalysts.[35–39] According to the earlier literatures, the promotional effect leads to a change in the metal environment upon promotion indicating an electronic and physical effect in nature, which is responsible for the improvement in the reduction and hydrogen adsorption capacity. Naturally from Figure 5 we can see the facility for the reduction of Pd nanoparticles on the Pd/HT_C-Al_2O_3 sample.

H_2-TPD experiments are performed in order to obtain the quantitative determination of the amount of chemisorbed hydrogen; it is a detailed indication of the degree of metal dispersion. The relevant dispersion properties calculated from desorption measurements on the series of catalysts are given in Table 1. The Pd loading in the three catalyst samples was very similar. The Pd dispersion in Pd/HT_C-Al_2O_3 was significantly higher than that in Pd/Al_2O_3 and Pd/HT_C-Al_2O_3. Based on the aforementioned results, it is concluded that by utilizing of the feature of hydrotalcite surface, we can improve the distribution of Pd particles and reduce the particle size for Pd catalysts by deposition of the Pd component on the hydrotalcite-modified porous alumina spheres.

Catalytic selective hydrogenation of DMT to DMCD

The selective hydrogenation of DMT to DMCD was carried out using Pd/HT_C-Al_2O_3, Pd/Al_2O_3 and Pd-Mg/Al_2O_3, with similar Pd loading, as catalyst under a variety of reaction conditions. The influence of reaction pressure on the catalytic performance of the three Pd catalyst samples is shown in Figure 6. Significantly, Pd/HT_C-Al_2O_3 exhibits the highest DMT conversion and DMCD selectivity over the employed pressure range between 3 MPa and 8 MPa. In despite of the decrease of reaction pressure the DMT conversion and DMCD selectivity for the Pd/HT_C-Al_2O_3 catalyst can keep running at high value, however, for the Pd/Al_2O_3 and Pd-Mg/Al_2O_3 samples, the DMT conversion and DMCD selectivity remarkably increase with the raise of reaction pressure. The byproducts identified by mass spectra are

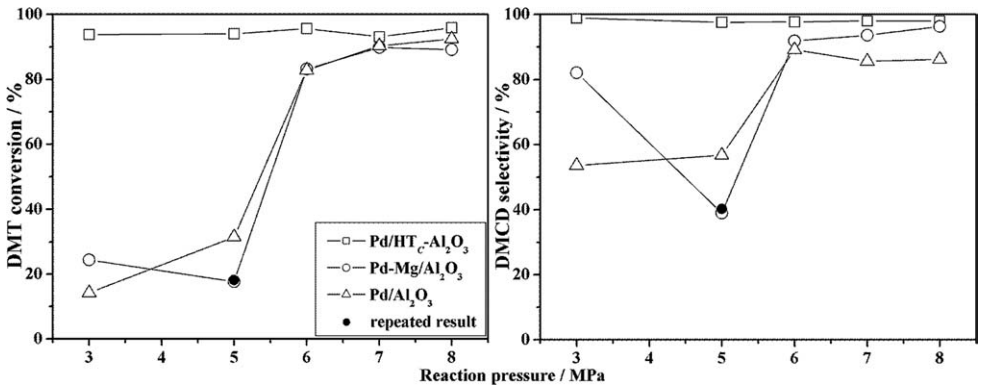

Figure 6. Influence of reaction pressure on the catalytic performance over three Pd catalysts.

The other reaction conditions: reaction temperature 225°C, hydrogen/DMT molar ratio 120, reaction time 6 h.

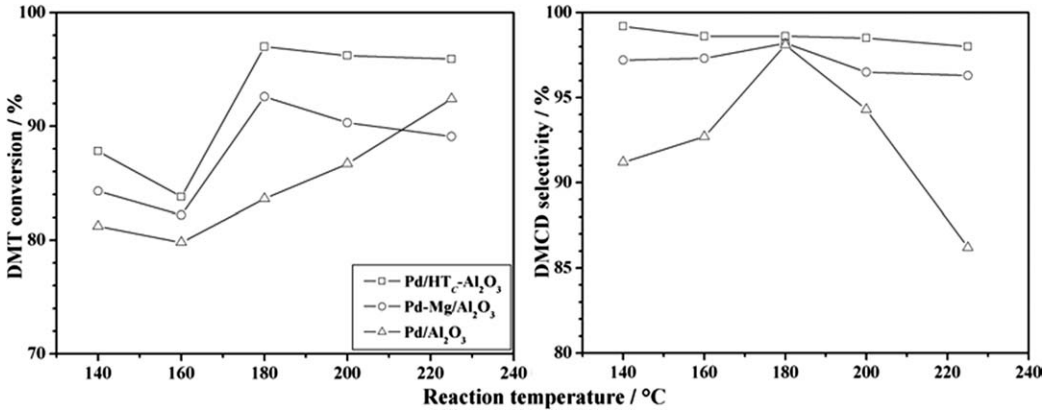

Figure 7. Influence of reaction temperature on the catalytic performance over three Pd catalysts.

The other reaction conditions: reaction pressure 8 MPa, hydrogen/DMT molar ratio 120, reaction time 6 h.

mainly 4-methyl-1-cyclohexanecarboxylate and trace 4-methyl-1-methyl benzecarboxylate. Furthermore, the catalytic performance of Pd-Mg/Al_2O_3 is generally superior to Pd/Al_2O_3, especially for the DMCD selectivity. However, at 5 MPa, the DMT conversion and DMCD selectivity for Pd-Mg/Al_2O_3 is lower than Pd/Al_2O_3. The Pd-Mg/Al_2O_3 catalyst with the same volumes was repeatedly operated at 5 MPa reaction pressure and the result is shown in Figure 6. We can see that the DMT conversion and DMCD selectivity retain the similar in each case.

As depicted in Figure 7, varying the reaction temperature plays an important role in the performance of Pd catalysts for selective hydrogenation of DMT to DMCD over the three Pd catalysts. It was observed that Pd/HT_C-Al_2O_3 exhibit the highest DMT conversion and DMCD selectivity at each employed reaction temperature. Furthermore, the DMT conversion first decreased with temperature increasing from 140 to 160°C. It is well-known that the reaction rate of hydrogenation is related to the partial pressure of both reactant and hydrogen.[40] According to Neri et al.[41] who studied hydrogenation of phenol to cyclohexanone over Pd and alkali-doped Pd catalysts, the reaction mechanism may involve the adsorption of reactant on the sites of the support at the interface of the Pd metal particles.[41] Here, in the given region of reaction temperature between 140 to 160°C, which is on the verge of the melting point (ca. 141°C) of DMT, the increased temperature could take some benefit for the adsorption of reactant DMT. However, it may simultaneously give rise to some more desorption of active hydrogen from the catalyst surface. Figure 7 shows that, beyond the region above, the DMT conversion underwent an increase with increase in reaction temperature to 180°C. Further increases in reaction temperature, however, caused the Pd/HT_C-Al_2O_3 and Pd-Mg/Al_2O_3 samples the slight decrease in DMT conversion again. Besides, we can see that from Figure 7 that for the Pd/HT_C-Al_2O_3 and Pd-Mg/Al_2O_3 samples, the DMCD selectivity slightly decrease with the raise of reaction temperature. However, the Pd/Al_2O_3 sample shows the highest DMCD selectivity, 98.1%, at reaction temperature 180°C. Thus, a reaction temperature of 180°C may be optimal for selective hydrogenation of DMT over the employed catalysts.

Furthermore, the terms of turnover frequency (TOF) values corresponding to the above employed conditions have been used in the comparison of DMCD yield of the three supported Pd catalysts (Figures 8 and 9). With the definition

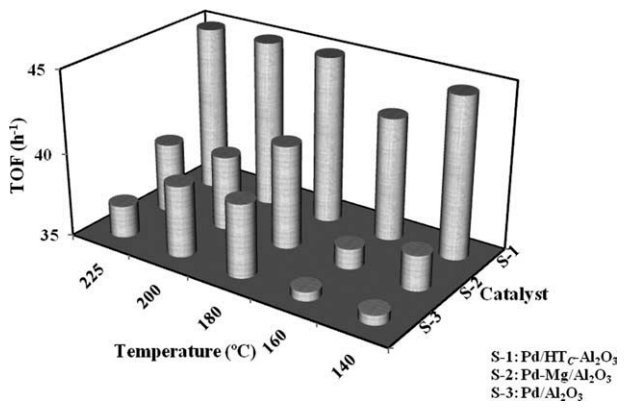

Figure 8. Turnover frequency (TOF) for production of DMCD from selective hydrogenation of DMT.

The other reaction conditions: reaction pressure 8 MPa, hydrogen/DMT molar ratio 120.

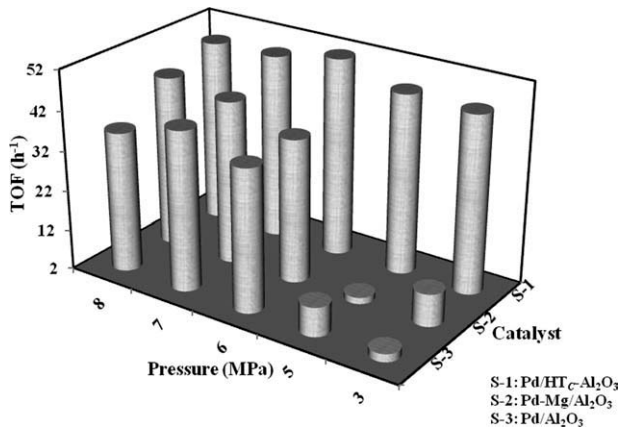

Figure 9. Turnover frequency (TOF) for production of DMCD from selective hydrogenation of DMT.

The other reaction conditions: reaction temperature 225°C, hydrogen/DMT molar ratio 120.

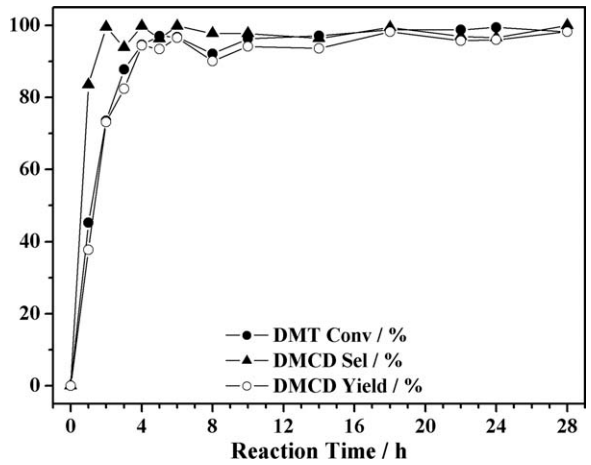

Figure 10. Time-on-stream analysis for the selective hydrogenation of DMT over Pd/HT_C-Al_2O_3 catalyst.

The reaction conditions: reaction pressure 8 MPa, reaction temperature 180°C, and hydrogen/DMT molar ratio 120.

of the number of molecules of DMCD produced per Pd atoms per hour, the TOF of DMCD yield is calculated as follows

$$\mathrm{TOF} = \frac{\textit{the number of moles of DMCD produced per hour yeild}}{\textit{the number of moles of supported Pd sites}}$$

where the number of supported Pd sites is assumed to be equal to the fractional number determined by exact ICP results. Obviously, at each employed condition, the TOF was higher for the designed Pd/HT_C-Al_2O_3 catalyst than for the two other Pd supported catalysts, especially at the mild reaction conditions.

The evaluation of reaction stability over Pd/HT_C-Al_2O_3 was carried out. Figure 10 reveals that the Pd/HT_C-Al_2O_3 sample exhibited excellent stability, retaining about 96.0% conversion of DMT, 98.5% selectivity of DMCD, and 95.0% yield of DMCD after reaction time 28 h. Furthermore, the Pd loading of the used catalyst was determined by ICP, which illustrated that no evident leaching of Pd after the reaction.

Figure 11 shows a representative HRTEM image of Pd/HT_C-Al_2O_3 after reaction. The Pd particles remained high dispersion with particle size of about 4 nm after reaction, which may be ascribed to the stable immobilization of Pd nanoparticles on the modified HT_C-Al_2O_3 support. The observed high-catalytic activity and selectivity and stability of Pd/HT_C-Al_2O_3 samples are consistent with its high and stable dispersion of Pd nanoparticles with small nanoparticle size,[33,42–44] resulting from the optimized loading on the modified support.

Conclusions

In summary, the spherical θ-Al_2O_3, with specific surface area and well-developed pores, was used as initial catalyst support and sole Al source for the *in situ* growth of MgAl-LDHs on the inner and outer surfaces, and then a new heterogeneous catalyst Pd/HT_C-Al_2O_3 was successfully prepared by wet impregnating method using the modified θ-alumina as support. Low-temperature N_2 adsorption-desorption experiments indicates that compared with the Pd/Al_2O_3 and Pd-Mg/Al_2O_3 samples prepared using unmodified θ-alumina as supports, Pd/HT_C-Al_2O_3 has slightly higher surface area and smaller most probable pore size. HRTEM demonstrates the presence of highly dispersed Pd nanoparticles with small particle size of about 4 nm in the Pd/HT_C-Al_2O_3 sample. H_2-TPR experiments illustrate that the Pd/HT_C-Al_2O_3 sample with modified Al_2O_3 support has a single reduced temperature around 47.4°C; while for the Pd/Al_2O_3 the reduced temperature is ca.72.8°C. The Pd-Mg/Al_2O_3 sample, however, has two reduction peaks at ca. 71.9°C and 56.2°C, respectively. The aforementioned results indicated the facility for the reduction of Pd nanoparticles on the Pd/HT_C-Al_2O_3 sample. Catalytic reactivity was investigated by using selective hydrogenation of DMT to DMCD. Pd/HT_C-Al_2O_3 shows a higher catalytic activity and selectivity and stability compared to Pd/Al_2O_3 and Pd-Mg/Al_2O_3 samples with the same loading of Pd and Mg prepared using unmodified θ-alumina as supports. The enhanced catalytic performance of the former material may be ascribed to its high dispersion of Pd nanoparticles and small particle size.

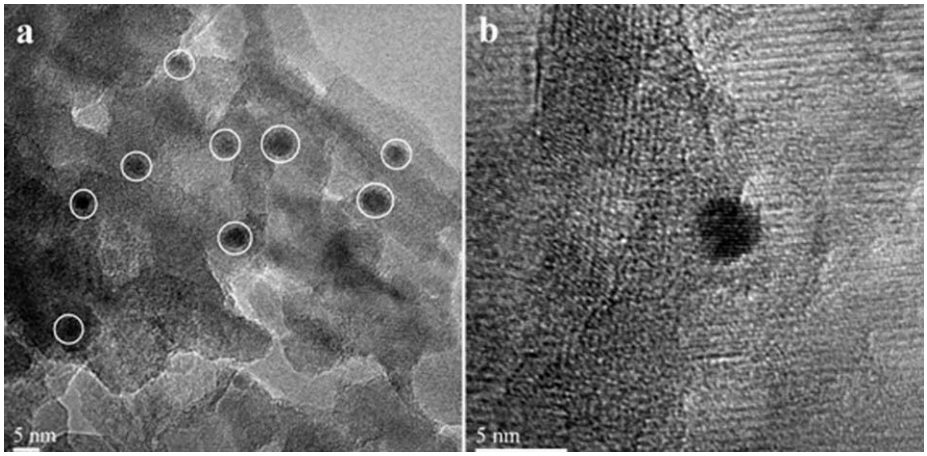

Figure 11. Representative HRTEM image of Pd/HT_C-Al_2O_3 (a) after reaction, and (b) shows a high-magnification view of (a).

Acknowledgments

We would like to thank Professor Dianqing Li at Beijing University of Chemical Technology who offered us the pristine alumina spheres and Professor Hui Zhang at Beijing University of Chemical Technology who helped us resolve some technique questions about the catalytic microreactor. This work was supported by the National Natural Science Foundation of China, the 973 Program (No. 2011CBA00506), and the Program for New Century Excellent Talents in Universities (No. NCET-07-0055).

Literature Cited

1. Turner SR. Development of amorphous copolyesters based on dimethanol. *Poly Sci*. 2004;42:5847.
2. Schlossman, Mitchell L. Universal nail polish using polyester resin. US patent US 4301046. November 17, 1981.
3. Appleton, Paul, Wood, and Michael A. Process. 1995, US patent 5414159. May 9, 1995.
4. Raja R, Khimyak T, Thomas JM, Hermans S, Johnson BFG. Single-step, highly active, and highly selective nanoparticle catalysts for the hydrogenation of key organic compounds. *Angew Chem Int Ed*. 2001;40:4638–4642.
5. Hungria AB, Raja R, Adama RD, Captain B, Thomas JM, Midegley PA, Golovko V, Johnson BFG. Single-step conversion of dimethyl terephthalate into cyclohexanedimethanol with Ru_5PtSn, a trimetallic nanoparticle catalyst. *Angew Chem Int Ed*. 2006;45:4782–4785.
6. Bond GC. *Catalysis by Metals*. New York: Academic Press; 1962:281–309.
7. Lam WK, Lioyd L. Catalyst selective hydrogenation of acetylene. *Oil Gas J*. 1972;27:66.
8. Toebes ML, Van Dillen JA, De Jong KP. Synthesis of supported palladium catalyst. *J Mole Catal A:Chem*. 2001;173:75–98.
9. Jiao L, Regalbuto JR. The synthesis of highly dispersed noble and base metals on silica via strong electrostatic adsorption: II. Mesoporous silica SBA-15. *J Catal*. 2008;260:342–350.
10. Zhang FX, Chen JX, Zhang X, Gao WL, Jin RC, Guan NJ. Simple and low-cost preparation method for highly dispersed Pd/TiO2 catalysts. *Catal Today*. 2004;93–95:645–650.
11. Lang YQ, Wang QQ, Xing JM, Zhang B, Liu HZ. Preparation of magnetic γ- Al_2O_3 supported palladium catalysts for hydrogenation of nitrobenzene. *AIChE J*. 2008;54:2303–2309.
12. Gareth RW, Dermot O'Hare. Towards understanding, control and application of layered double hydroxide chemistry. *J Mater Chem*. 2006;16:3065.
13. Evans DG, Duan X. Preparation of layered double hydroxides and their applications as additives in polymers, as precursors to magnetic materials and in biology and medicine. *Chem Commun*. 2006;485:485–496.
14. Cavani F, Trifiro F, Vaccari A. Hydrotalcite-type anionic clays: Preparation, properties and applications. *Catal Today*. 1991;11:173.
15. Vaccari A. Clays and catalysis: a promising future. *Appl Clay Sci*. 1999;14:161–198.
16. Sels BF, De Vos DE, Jacobs PA. Hydrotalcite-like anionic clays in catalytic organic reactions. *Catal Rev Sci Eng*. 2001;43:443–488.
17. Tichit D, Coq B. Catalysis by hydrotalcite and related materials. *Cattech*. 2003;7:206–217.
18. Zhang FZ, Xiang X, Li F, Duan X. Layered double hydroxides as catalytic materials: recent developments. *Catal Surv Asia*. 2008:2; 253–265.
19. Ken M, Daisuke N, Kohsuke M, Tomoo M, Kohki E, Kiyotomi K. A ruthenium- grafted hydrotalcite as a multifunctional catalyst for direct α-alkylation of nitriles with primary alcohols. *J Am Chem Soc*. 2004;126:5662–5663.
20. Kohki E, Ken M, Tomoo M, Klyotomi K. Heterotrimetallic RuMnMn Species on a hydrotalcite surface as highly efficient heterogeneous catalysts for liquid-phase oxidation of alcohols with molecular oxygen. *Angew Chem Int Ed*. 2005;44:3423–3426.
21. Kapoor MP, Yasuyuki M. Liquid phase methanol carbonylation catalysed over rhodium supported on hydrotalcite. *Chem Commun*. 2000;36:95–96.
22. Meshesha BT, Chimenta RJ, Medina F, Sueiras JE, Cesteros Y, Salagre P, Figueras F. Catalytic hydrodechlorination of 1,2,4-trichlorobenzene over Pd/Mg (Al)O catalysts. *Appl Catal B Environ*. 2009;87:70–77.
23. Li F, Duan X. Structural aspects of layered double hydroxides. *Struct Bond*. 2006;119:193.
24. Basile F, Vaccari A, Rives V. *Layered Double Hydroxides: Present and Future*. New York: Nova Science Publishers; 2001.
25. Xiang X, Bai L, Li F. Formation and catalytic performance of supported Ni nanoparticles via self-reduction of hybrid NiAl-LDH/C composite. *AIChE J*. 2010;56:2934–2945.
26. Paulhiac JL, Clause O. Surface coprecipitation of Co(II), Ni(II), or Zn(II) with Al(III) ions during impregnation of γ-alumina at neutral pH. *J Am Chem Soc*. 1993;115:11602–11603.
27. Jean-Baptiste d'Espinose de la C, Maggy K, Oliver C. Impreganation of γ- alumina with Ni(II) or Co(II) ions at neutral pH: hydrotalcite-type coprecipitate formation and characterization. *J Am Chem Soc*. 1995;117:11471–11481.
28. Feng JT, Lin YJ, Evans DG, Duan X, Li DQ. Enhanced metal dispersion and hydrodechlorination properties of a Ni/Al2O3 catalyst derived from layered double hydroxides. *J Catal*. 2009;266:351–358.
29. Mok KB, Ross JRH, Sambrook RM, Poncelet G, Grange P, Jacobs PA. *Preparation of Catalysts III*. Amsterdam: Elsevier; 1983:291.
30. Mario AP, Claude F, Jean PB. Synthesis of Al-rich hydrotalcite-like compounds by using the urea hydrolysis reaction-control of size and morphology. *J Mater Chem*. 2003;13:1988–1993.
31. Chen YZ, Liaw CW, Lee L. Selective hydrogenation of phenol to cyclohex-anone over palladium supported on calcined Mg/Al hydrotalcite. *Appl Catal A*. 1999;177:1–8.
32. Gregg SG, Sing KSW. *Adsorption, Surface Area and Porosity*. New York: Academic Press; 1982.
33. Feng JT, Wang HY, Evans DG, Duan X, Li DQ. Catalytic hydrogenation of ethyl anthraquinone over highly dispersed eggshell Pd/SiO_2-Al_2O_3 spherical catalysts. *Appl Catal A*. 2010;382:240–245.
34. Aamir IK, Dermot O'Hare. Intercalation chemistry of layered double hydroxides: recent development and applications. *J Mater Chem*. 2002;12:3191–3198.
35. Gotti A, Prins R. Basic metal oxides as co-catalysts in the conversion of syn-thesis gas to methanol on supported palladium catalysts. *J Catal*. 1998;175:302–311.
36. Gusovius AF, Walting TC, Prins R. Ca promoted Pd/SiO_2 catalysts for the syn-thesis of methanol from CO: the location of the promoter. *Appl Catal A*. 1999;188:187–199.
37. Gusovius AF, Prins R. Alloy formation in Li-promoted Pd/SiO_2 catalysts for the synthesis of methanol. *J Catal*. 2002;211:273–277.
38. Unnikrishnan RP, Endalkachew SD. Strontium as an efficient promoter for supported palladium hydrogenation catalysts. *Appl Catal A*. 2005;281:31–38.
39. Emerson AS, Jose J, Mario de JM, Francois BV. Palladium, palladium-tin, and palladium-silver catalysts in the selective hydrogenation of hexadienes: TPR, mössbauer, and infrared studies of adsorbed CO. *J Catal*. 2000;195:88–95.
40. Antonymuthu S, Barry HC. Aromatic hydrogenation catalysis: A review. *Catal Rev Sci Eng*. 1994:36:78–97.
41. Neri G, Visco AM, Donato A, Milone C, Malentacchi M, Gubitosa G. Hydrogenation of phenol to cyclohexanone over palladium and alkali-doped palladium catalysts. *Appl Catal A*. 1994;110:49–59.
42. Agnes M, Zolatan K. Pd nanoparticles in hydrotalcite: mild and highly selective catalysts for alkyne semihydrogenation. *J Catal*. 2003;220:372–381.
43. Hari PA, Venugopal A, Krishnamurthy J, Seetha Rama RK, Kanto Rao Panja K G, Niemantsverdriet JW. Characterization and reactivity of Pd/MgO and Pd/γ- Al_2O_3 catalysts in the selective hydrogenolysis of CCl_2F_2. *J Phy Chem B*. 2002;106:1024–1031.
44. Duraiswami D, Dhanagopal M, Valentine R, Esther LP, Revathi C, Thiripuran Thiripuranthagan S. Palladium-nanoparticle intercalated vermiculite for selective hydrogenation of α,β-unsaturated aldehydes. *J Chem Technol Biotechnol*. 2007;82:253–258.

Manuscript received Feb. 23, 2011, and revision received May 19, 2011.